

# Cardiac magnetic resonance–derived myocardial scar is associated with echocardiographic response and clinical prognosis of left bundle branch area pacing for cardiac resynchronization therapy

Zhongli Chen <sup>1†</sup>, Xuan Ma <sup>2†</sup>, Yuan Gao <sup>1</sup>, Sijin Wu <sup>1</sup>, Nan Xu <sup>3</sup>,  
Feng Chen <sup>1</sup>, Yanyan Song <sup>2</sup>, Chongqiang Li<sup>4</sup>, Minjie Lu <sup>2</sup>, Yan Dai<sup>1</sup>,  
Michael R. Gold <sup>5</sup>, Shihua Zhao <sup>2\*</sup>, and Keping Chen <sup>1\*</sup>

<sup>1</sup>State Key Laboratory of Cardiovascular Disease, Cardiac Arrhythmia Center, Fuwai Hospital, National Center for Cardiovascular Disease, Chinese Academy of Medical Sciences and Peking Union Medical College, No. 167 North Lishi Rd, Xicheng District, Beijing 100037, China; <sup>2</sup>Department of Magnetic Resonance Imaging, National Center for Cardiovascular Diseases, Fuwai Hospital, Chinese Academy of Medical Sciences and Peking Union Medical College, No. 167 North Lishi Rd, Xicheng District, Beijing 100037, China; <sup>3</sup>Department of Echocardiography, National Center for Cardiovascular Diseases, Fuwai Hospital, Chinese Academy of Medical Sciences and Peking Union Medical College, No. 167 North Lishi Rd, Xicheng District, Beijing 100037, China; <sup>4</sup>Catheterization Laboratory, National Center for Cardiovascular Diseases, Fuwai Hospital, Chinese Academy of Medical Sciences and Peking Union Medical College, No. 167 North Lishi Rd, Xicheng District, Beijing 100037, China; and <sup>5</sup>Division of Cardiology, Medical University of South Carolina, Charleston, SC, USA

Received 24 August 2023; accepted after revision 28 October 2023; online publish-ahead-of-print 31 October 2023

## Aims

Left bundle branch area pacing (LBBAP) is a novel approach for cardiac resynchronization therapy (CRT), but the impact of myocardial substrate on its effect is poorly understood. This study aims to assess the association of cardiac magnetic resonance (CMR)–derived scar burden and the response of CRT via LBBAP.

## Methods and results

Consecutive patients with CRT indications who underwent CMR examination and successful LBBAP-CRT were retrospectively analysed. Cardiac magnetic resonance late gadolinium enhancement was used for scar assessment. Echocardiographic reverse remodelling and composite outcomes (defined as all-cause death or heart failure hospitalization) were evaluated. The echocardiographic response was defined as a  $\geq 15\%$  reduction of left ventricular end-systolic volume. Among the 54 patients included, LBBAP-CRT resulted in a 74.1% response rate. The non-responders had higher global, septal, and lateral scar burden (all  $P < 0.001$ ). Global, septal, and lateral scar percentage all predicted echocardiographic response [area under the curve (AUC): 0.857, 0.864, and 0.822; positive likelihood ratio (+LR): 9.859, 5.594, and 3.059; and negative likelihood ratio (–LR): 0.323, 0.233, and 0.175 respectively], which was superior to QRS morphology criteria (Strauss left bundle branch abnormality: AUC: 0.696, +LR 2.101, and –LR 0.389). After a median follow-up time of 20.3 (11.5–38.7) months, higher global, lateral and septal scar burdens were all predictive of the composite outcome (hazard ratios: 4.996, 7.019, and 4.741, respectively;  $P$ 's  $< 0.05$ ).

## Conclusion

Lower scar burden was associated with higher response rate of LBBAP-CRT. The pre-procedure CMR scar evaluation provides further useful information to identify potential responders and clinical outcomes.

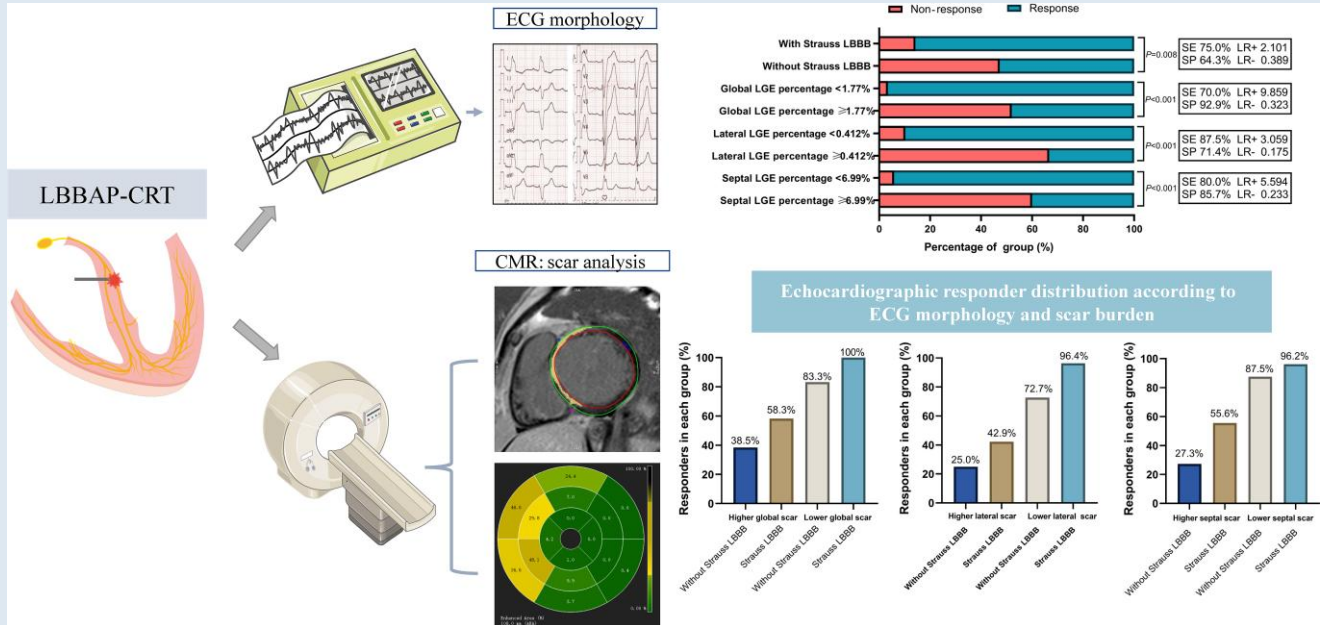
\* Corresponding authors. Tel: +86 010 88392295. E-mail address: chenkeping@263.net (K.C.); Tel: +86 010 88398408. E-mail address: cjrzhaojihua2009@163.com (S.Z.);

† The first two authors contributed equally to the study.

© The Author(s) 2023. Published by Oxford University Press on behalf of the European Society of Cardiology.

This is an Open Access article distributed under the terms of the Creative Commons Attribution License (<https://creativecommons.org/licenses/by/4.0/>), which permits unrestricted reuse, distribution, and reproduction in any medium, provided the original work is properly cited.

## Graphical Abstract



Cardiac magnetic resonance–derived myocardial scar predicts response of cardiac resynchronization therapy via left bundle branch area pacing. Baseline electrocardiogram morphology and pre-procedural scar evaluation from cardiac magnetic resonance predict reverse remodelling after left bundle branch area pacing for cardiac resynchronization therapy. Low global, septal, and lateral scar burden helps to identify more responders on top of Strauss left bundle branch abnormality.

### Keywords

LBBAP • CMR • Scar • Cardiac resynchronization • Response

### What's new?

- Global, septal, and lateral scar burdens in the left ventricle correlated negatively with reverse remodelling and displayed better performance beyond left bundle branch abnormality for predicting echocardiographic response in patients who underwent left bundle branch area pacing for cardiac resynchronization therapy (LBBAP-CRT).
- Measures of myocardial scar were also strong predictors of clinical outcomes after LBBAP-CRT.
- Pre-procedure cardiovascular magnetic resonance for myocardial scar evaluation may offer values to improve the selection of LBBAP-CRT candidates and optimize clinical decision-making.

## Introduction

Cardiac resynchronization therapy (CRT) with traditional biventricular pacing (BVP) is an established effective therapy for patients with heart failure (HF) with a reduced ejection fraction (EF) and QRS prolongation, despite optimal medical therapy. There is a 30–40% non-responding rate using traditional criteria,<sup>1,2</sup> although the classification of response remains controversial.<sup>3,4</sup> More recently, techniques have been developed to perform left bundle branch area pacing (LBBAP), as a rescue or alternative for BVP.<sup>5,6</sup> Through recruitment of the intrinsic left ventricular (LV) conduction system, LBBAP can also achieve improved electrical and mechanical synchrony, especially in patients with left bundle branch abnormality (LBBB).<sup>7</sup> Multicentre studies have reported both acute and long-term safety and efficacy of this approach.<sup>5,8</sup> More recently, a prospective, randomized trial (LBBP-RESYNC) with a head-to-head comparison of LBBAP-CRT and

BVP-CRT showed LBBAP as a promising alternative to traditional CRT. There was greater LVEF improvement compared with BVP-CRT among patients with LBBB and non-ischaemic HF.<sup>9</sup>

In contrast to BVP-CRT, there are still no tailored criteria for patient selection, and established evidence for response rate is limited. Based on standard BVP-CRT selection criteria, such as LV systolic dysfunction, prolonged QRS duration (QRSd), and LBBB morphology, the non-responder rate for LBBAP-CRT ranges from 10 to 30%.<sup>3,10,11</sup> Apart from these clinical parameters noted above, pre-procedure imaging evaluation of LV was considered an important quality indicator to improve the care and outcomes of cardiac pacing<sup>12</sup>; however, limited data exist regarding the imaging evaluation in relation to the LBBAP-CRT response and HF prognosis.

Cardiovascular magnetic resonance (CMR) by late gadolinium enhancement (LGE) is a well-established and accurate approach for localizing and quantifying myocardial scar. In BVP-CRT, scar in the LV pacing site has been associated with adverse outcomes following implantation.<sup>13</sup> However, the effect of the scar on LBBAP-CRT acute response and prognosis is unknown. Moreover, since LBBAP is commonly achieved through deep septal penetration, so there is concern that septal scar may be detrimental on the response of LBBAP-CRT. A recent study indicates that CMR helps in predicting the procedural failure of LBBAP among patients with extensive LV scar burden.<sup>14</sup> Data from computer simulations predict that septal scar may also have an adverse impact on LBBAP-CRT response.<sup>15</sup> However, there is a paucity of clinical data concerning the prognostic impact of CMR-LGE for LBBAP among HF patients with CRT indications. Accordingly, in the present study, the impact of scar features on LBBAP-CRT response was evaluated including acute and more long-term clinical outcomes.

## Methods

### Study population

This was a retrospective, single-centre study. Consecutive patients were enrolled from January 2019 to March 2022, who had New York Heart Association (NYHA) functional classes II–IV, HF symptoms despite optimal guideline-directed medical therapy, baseline LVEF  $\leq 35\%$  with indications for CRT or baseline LVEF  $< 50\%$  with expected high ventricular pacing burden  $> 40\%$ ,<sup>16,17</sup> and underwent CMR examination (cine and contrast) prior to the CRT implantation within 3 months of implantation. Exclusion criteria were listed as follows: (i) age  $< 18$  years, (ii) life expectancy  $< 12$  months, (iii) pre-existing CRT devices or pacemakers, (iv) without available pre-procedural CMR examination in our centre, and (v) CMR image quality not allowing accurate LGE analysis. A flow chart of patients meeting exclusion criteria is presented in [Supplementary material online, Figure S1](#).

In our centre, for patient indicated for CRT who had LBBB morphology or with expected high ventricular pacing percentage, LBBAP was mainly taken as a primary strategy. For the CRT candidates with prolonged QRSd but did not meet the LBBB criteria, BVP was often preferred as the primary strategy, with LBBAP serving as a rescue approach. Patients with successful LBBAP as a primary CRT approach ( $n = 43$ ) or rescue approach ( $n = 11$ ) to failed BVP because of difficult coronary sinus (CS) lead placement or high capture threshold comprised the study population. The pre-procedure standard clinical information including NYHA functional class, comorbidities, medication therapy, serum blood test results, and echocardiographic assessment were collected. In this study, LBBB was defined according to the Strauss criteria, as QRSd  $> 140$  ms in men ( $> 130$  ms in women) and the presence of at least two mid-QRS notches or slurs in leads I, aVL, V1, V2, V5, and V6.<sup>18</sup> The study conforms to the Helsinki Declaration guidelines and was approved by the Fuwai Hospital Institutional Review Board and Ethical Committee (Approval No. 2019-1149). All patients provided informed consent for the procedure.

### Procedure details and device programming

Left bundle branch area pacing implantation was performed as previously described.<sup>10</sup> In brief, the SelectSecure pacing lead (Model 3830 69 cm, Medtronic Inc., Minneapolis, MN, USA) was introduced in the right ventricle through the fixed-curve sheath delivery system (C315 HIS, Medtronic Inc., Minneapolis, MN, USA) under the fluoroscopic right anterior oblique  $30^\circ$ . The lead was advanced into the ventricular septum from the right side of interventricular septum towards the LBB area. Real-time 12-lead electrocardiograms (ECG) and intracardiac electrograms were recorded during the procedure and pacing tests. QRS morphology was monitored, and the pacing stimulus to R wave peak time (stim-RWPT) in lead V6 was measured at both low and high output. Left bundle branch capture was considered present according to previous definitions.<sup>5,19,20</sup>

For those patients implanted with a CRT-pacemaker (CRT-P) device ( $n = 16$ ), the 3830 lead was connected to the right ventricular (RV) port, with the CS lead connecting to the LV port as a backup. For those implanted with a CRT-defibrillator (CRT-D) device, the 3830 lead was connected to the LV port, and the defibrillator lead was connected to the RV port. The atrioventricular (AV) and/or interventricular (VV) delay was optimized to ensure the narrowest QRS complex in LBBAP-CRT. If the electrical correction was favourable by LBBAP, the CS-LV lead was inactivated allowing for LBBAP alone. Four patients received LBBAP and LV pacing (LOT-CRT) due to unfavourable electrical resynchronization.

### Cardiovascular magnetic resonance acquisition

Standard CMR was performed on 3.0-T scanners (Discovery MR750W, GE Healthcare, Milwaukee, WI; Ingenia, Philips Healthcare, Best, The Netherlands; or Skyra, Siemens, Erlangen, Germany) with a phased-array cardiac coil and retrospective electrocardiographic gating. Cine images using balanced steady-state free precession (bSSFP) were acquired in three long-axis planes (LV outflow tract, two- and four-chamber view) and in sequential short-axis slices from the atrioventricular ring to the LV apex.

### Cardiovascular magnetic resonance analysis

All CMR images were uploaded and analysed using commercial post-processing software CVI42 (version 5.12.4, Circle Cardiovascular Imaging, Calgary, Canada). The images were reviewed separately by two radiologists (Y.S. and X.M.) who were blinded to the clinical information or outcomes and adjudicated by the senior radiologist (S.Z.) to minimize the difference.

For LV deformation analysis, end-diastolic endo- and epicardial contours were traced semi-automatically with manual adjustment in long-axis views and short-axis views on cine images.<sup>21</sup> Late gadolinium enhancement images were first reviewed for visible LGE (areas with relatively increased signal intensity following administration of gadolinium contrast), and if positive, its location and pattern were categorized. The location was classified as septal, LV free wall, or as occurring in both locations. The pattern was classified as linear mid-wall, subepicardial, focal, or as occurring in multiple patterns. Late gadolinium enhancement quantification was performed by setting the signal intensity threshold at 6 SD above the mean intensity of a reference region of myocardium that had no visual evidence of enhancement. The manual correction was performed for obvious threshold errors. The percentage of LGE is presented as the percentage of total LV mass (LGE%). In addition to global quantification of LGE at this level, segmental quantification was performed based on the American Heart Association 16-segment model after defining the reference point at RV insertion. The percentage of LGE in anteroseptal and anteroseptal (2, 3, 8, and 9) segments was used to calculate 'septal LGE%', while anterolateral and inferolateral (5, 6, 11, and 12) segments were used to calculate 'lateral LGE%'.

Further details of the LBBAP-CRT implantation and the CMR acquisition are presented in the [Supplementary material](#).

### Outcome definition and follow-up

All patients received routine clinic follow-ups at 6 months for NYHA functional class and echocardiographic indices. The primary echocardiographic response was defined as  $\geq 15\%$  LV end-systolic volume (LVESV) reduction in accordance with previous publications.<sup>22,23</sup> Super-response was defined as an absolute improvement of LVEF  $\geq 20\%$  or LVEF to  $\geq 50\%$  for patients with baseline LVEF  $\leq 35\%$ .<sup>5</sup> In addition, the percentage change in LVESV, LVEF, and LV end-diastolic diameter (LVEDD) were measured at baseline and 6 months. Clinical response at 6 months was defined as an improvement in NYHA functional class by at least one class and no HF hospitalization (HFH).<sup>24</sup> Patients were followed up for the composite outcome of any HFH or all-cause death by trained doctors on a regular phone interview or outpatient service. Heart failure hospitalization was defined as a hospital admission or an urgent care visit for intensive treatment for HF with intravenous diuretics or intravenous inotropic medications. The last follow-up time was in November 2022.

### Statistical analysis

Continuous variables were described as mean with standard deviation if normally distributed, otherwise as median with interquartile range (IQR). The discrete variables were depicted as counts and proportions. Student's *t*-test/Mann–Whitney *U* test was applied for evaluating the differences of continuous variables for appropriateness. The  $\chi^2$  test or Fisher's exact test was used for assessing the difference of discrete variables between groups. The correlation between imaging markers and the change of LVEDD, LVESV, and LVEF was examined by the Spearman correlation rank test and evaluated by the correlation coefficient and *P*-value. A stepwise multivariate linear regression model was used to estimate the contributions of clinical and CMR variables to LVEF improvement. The parameters included in the analysis were age, sex, baseline QRSd, baseline LVEDD, Strauss LBBB, QRSd reduction, stim-V6 RWPT at 3 V at 0.5 ms, the capture of LBB, comorbid atrial fibrillation, and estimated glomerular filtration rate (eGFR),<sup>5,25</sup> as well as CMR parameters.

The receiver operating characteristic (ROC) curves were performed to evaluate the discriminability of clinical and imaging markers for predicting echocardiographic response, clinical response, and super-response by using the highest Youden index (sensitivity + specificity – 1) to determine the optimal cut-off values for each imaging marker. The positive predictive value (PPV), negative predictive value (NPV), positive likelihood ratio (+LR), and negative likelihood ratio (–LR) were calculated. Kaplan–Meier curves were used to examine cumulative event rates following LBBAP-CRT, and the difference between groups was tested using a log-rank test. The hazard

**Table 1** Clinical characteristics

	All (n = 54)	Non-responders (n = 14)	Responders (n = 40)	P-value
Age, years	57.7 ± 11.5	55.4 ± 10.7	58.5 ± 11.8	0.392
Male, n (%)	29 (53.7%)	9 (64.3%)	20 (50%)	0.356
Comorbidities				
AF, n (%)	8 (14.8%)	4 (28.6%)	4 (10.0%)	0.092
Hypertension, n (%)	17 (31.5%)	3 (21.4%)	14 (35.0%)	0.347
CKD, n (%)	5 (9.3%)	2 (14.3%)	3 (7.5%)	0.595
ECG parameters				
Baseline QRS duration	166.8 ± 27.0	155.8 ± 35.8	170.6 ± 22.4	0.076
QRS complex morphology				0.027
LBBB (Strauss criteria)	35 (64.8%)	5 (35.7%)	30 (75.0%)	
IVCD	14 (25.9%)	7 (50.0%)	7 (17.5%)	
Narrow QRSd	5 (9.3%)	2 (14.3%)	3 (7.5%)	
Laboratory tests				
eGFR, mL/min	78.4 (68.8–92.1)	70.2 (51.1–85.7)	80.2 (69.4–92.8)	0.15
NT-proBNP, pg/mL	1350 (600.8–2719.1)	2699.2 (1375.2–3747.6)	1181.0 (544.5–2037.8)	0.013
LVEF, %	30 (26.2–35.0)	28.5 (27.0–32.0)	30.5 (26.0–35.0)	0.699
NYHA functional class				
II	13 (24.1%)	1 (7.1%)	12 (30.0%)	0.031
III	39 (72.2%)	11 (78.6%)	28 (70.0%)	
IV	2 (3.7%)	2 (14.3%)	0 (0.0%)	
Medical treatment				
ACE-I/ARB/ARNI, n (%)	51 (94.4%)	14 (100.0%)	37 (92.5%)	0.56
Beta blockers, n (%)	54 (100.0%)	14 (100%)	40 (100%)	–
Aldosterone antagonists, n (%)	53 (98.1%)	14 (100.0%)	39 (97.5%)	1
Diuretics, n (%)	53 (98.1%)	14 (100.0%)	39 (97.5%)	1
Digoxin, n (%)	21 (38.9%)	6 (42.9%)	15 (37.5%)	0.723
Type of device				
CRT-D, n (%)	38 (70.4%)	3 (21.4%)	13 (32.5%)	0.435
CRT-P, n (%)	16 (29.6%)	11 (78.6%)	27 (67.5%)	

ACE-I, angiotensin-converting enzyme inhibitor; AF, atrial fibrillation; ARB, angiotensin receptor blockers; ARNI, angiotensin receptor/neprilysin inhibitor; CKD, chronic kidney disease; CRT-D, cardiac resynchronization therapy-defibrillator; CRT-P, cardiac resynchronization therapy-pacemaker; eGFR, estimated glomerular filtration rate; LBBB, left bundle branch abnormality; LVEF, left ventricular ejection fraction; NT-proBNP, N-terminal pro-B-type natriuretic peptide; NYHA, New York Heart Association.

ratio (HR) was estimated using the univariate Cox proportional hazards model. All tests were two tailed with an  $\alpha$  level of 0.05 considered statistically significant. Statistical analyses were performed using R software version 4.1.2 and SPSS version 22 (IBM, Armonk, NY, USA).

## Results

### Patient characteristics

Fifty-four patients (mean age of 57.7 years old, 53.7% male) were included in this study, including 9 (16.7%) HF patients with expected high ventricular pacing burden due to AV block. Baseline characteristics and echocardiographic evaluation during follow-up of the cohort are summarized in [Table 1](#) and [Supplementary material online, Table S1](#), respectively. Most patients had non-ischaemic cardiomyopathy (NICM, 96.3%). Left bundle branch abnormality morphology meeting Strauss criteria was present in 35 (64.8%) patients, while the remaining 35.2% were composed of intraventricular conduction delay (IVCD;  $n = 14$ ) and narrow QRS complex ( $n = 5$ ). At 6 months follow-up, 40

(74.1%) and 35 (64.8%) patients have echocardiographic and clinical response, respectively, and there were 21 patients (38.9%) classified as super-responders. There was no significant difference in demographic features, pre-procedure LVEF, comorbidities, baseline QRSd, or medical treatment between the responders and non-responders. The patients in the non-response group were characterized by higher baseline N-terminal pro-B-type natriuretic peptide (NT-proBNP) levels, larger LV, advanced NYHA functional class, and without Strauss LBBB ECG morphology. Those with echocardiographic response were more likely to have evidence of LBB capture and a greater QRSd reduction (see [Supplementary material online, Table S1](#)).

### Cardiovascular magnetic resonance-derived scar features

Cardiovascular magnetic resonance parameters for the total study population, as well as echocardiographic responder, and non-responder subgroups are summarized in [Supplementary material online, Table S2](#).



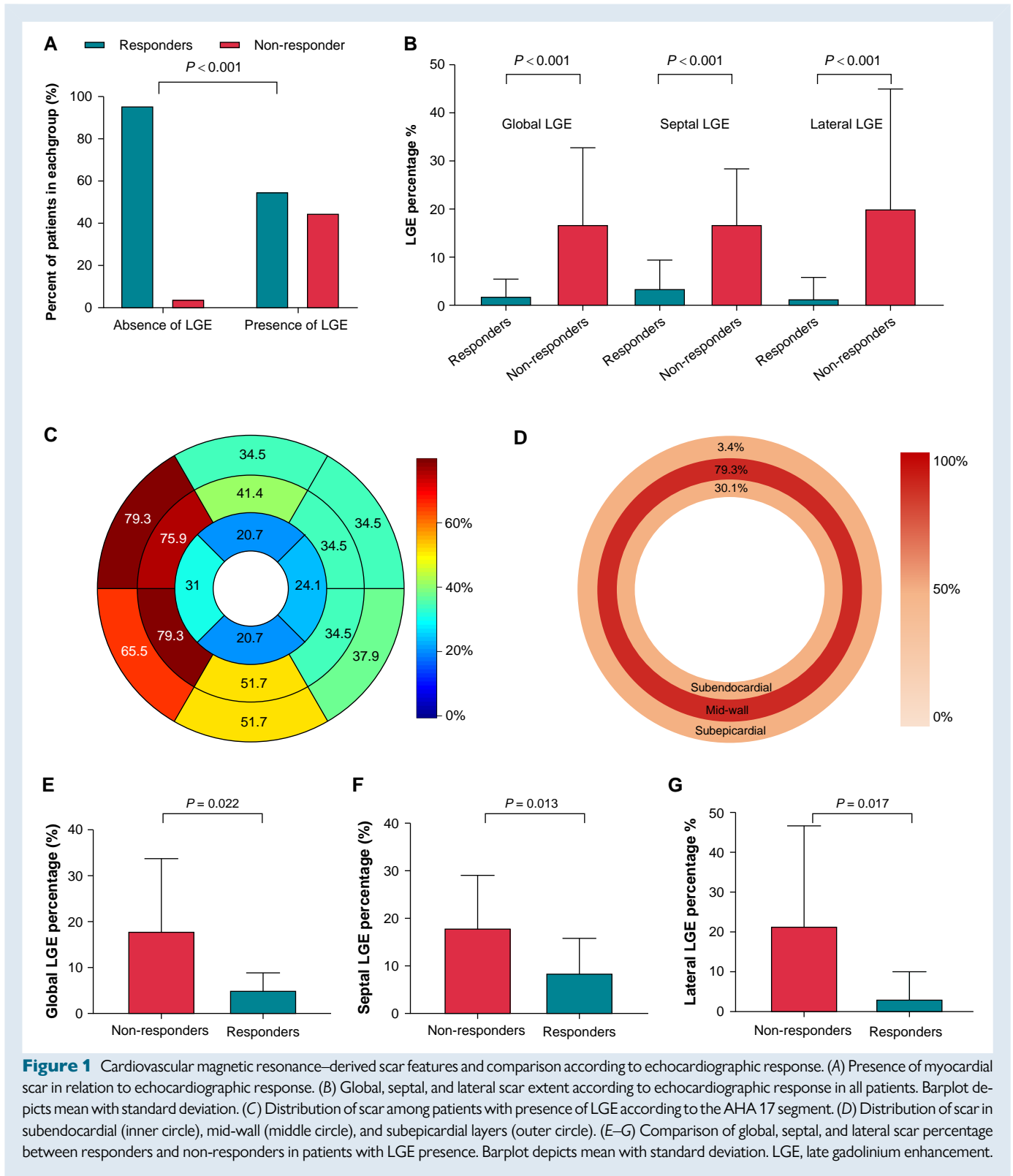
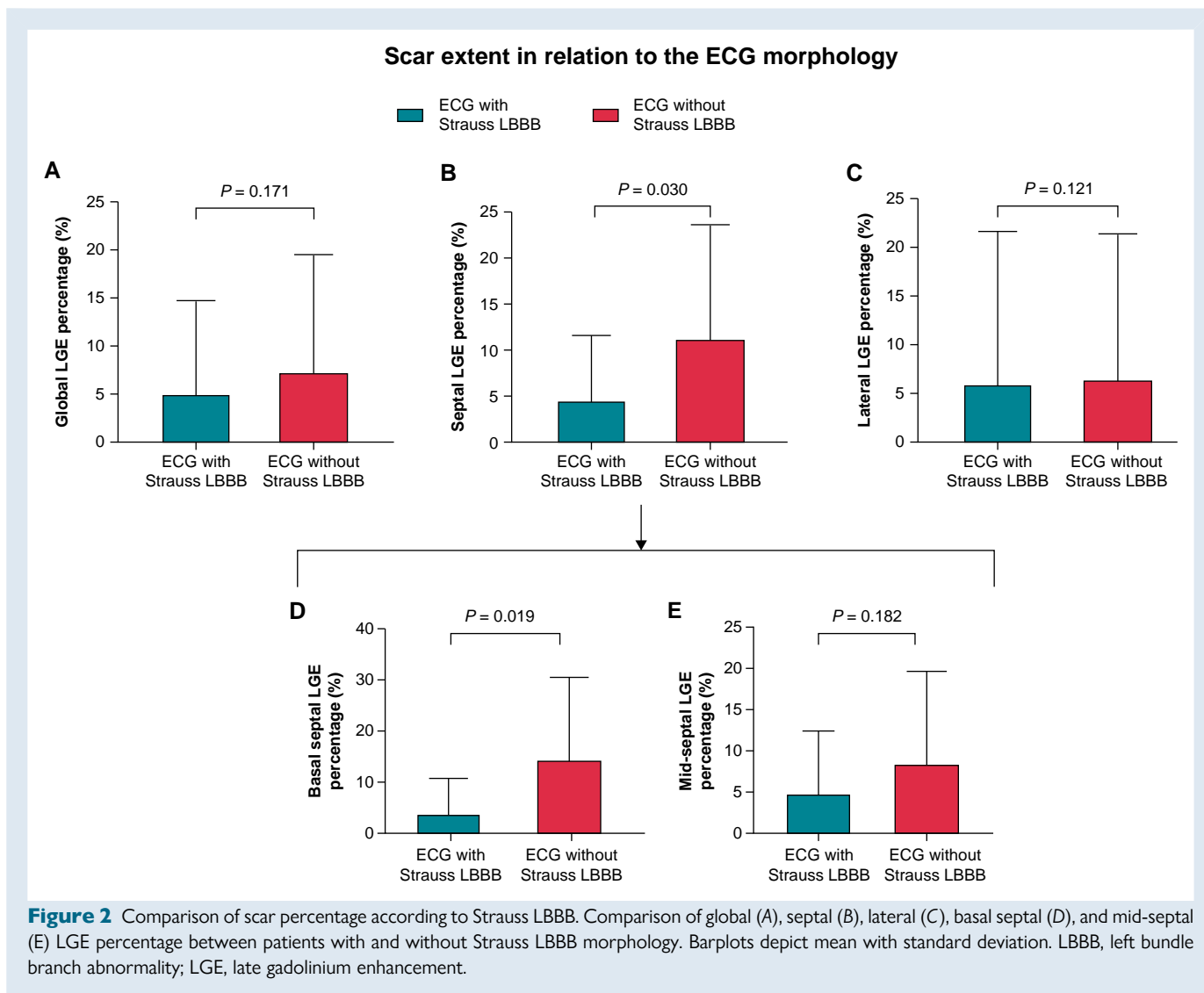


**Figure 1** Cardiovascular magnetic resonance–derived scar features and comparison according to echocardiographic response. (A) Presence of myocardial scar in relation to echocardiographic response. (B) Global, septal, and lateral scar extent according to echocardiographic response in all patients. Barplot depicts mean with standard deviation. (C) Distribution of scar among patients with presence of LGE according to the AHA 17 segment. (D) Distribution of scar in subendocardial (inner circle), mid-wall (middle circle), and subepicardial layers (outer circle). (E–G) Comparison of global, septal, and lateral scar percentage between responders and non-responders in patients with LGE presence. Barplot depicts mean with standard deviation. LGE, late gadolinium enhancement.

The basic CMR morphological parameters did not demonstrate a significant difference between the responders and non-responders. However, those without myocardial LGE had a higher echocardiographic response rate than those with the presence of LGE (response rate: 96.0% vs. 55.2%,  $P < 0.001$ ; Figure 1A). The median percentage of LGE between the responders and non-responders was significantly

different, with responders demonstrating lower global, septal, and lateral LGE percentage, as shown in Figure 1B and summarized in Supplementary material online, Table S2.

In 29 patients with myocardial scar, LGE localized in either free wall ( $n = 4$ ), septal ( $n = 13$ ), or both ( $n = 12$ ), and it was more commonly localized in septal segments ( $n = 25$ , 86.2%; Figure 1C). Patients with



combined septal and free-wall LGE displayed were more likely to be non-responders compared with those having LGE located in only one area ( $P = 0.006$ ). Mid-wall LGE was the most common pattern found in the study population, which was observed in 23 patients (79.3%; Figure 1D). Among the patients with myocardial scars, global scar percentage [median (IQR) responders: 5.1% (2.0–7.0%) vs. non-responders: 16.6% (4.3–27.0%),  $P = 0.022$ ], lateral scar percentage [median (IQR): responders 0.1% (0.0–1.8%) vs. non-responders: 8.6% (0.7–39.7%),  $P = 0.017$ ] and septal scar percentage [median (IQR): responders 7.4% (3.8–11.8%) vs. non-responders: 17.3% (8.8–22.2%),  $P = 0.013$ ] were also significantly lower in responders than the non-responders (Figure 1E–G). The non-responders held significantly higher scar percentage in basal septal segments ( $P = 0.028$ ) and higher scar percentage with a trend toward significance in mid-septal segments ( $P = 0.059$ ).

### Association between scar burden, electrocardiogram morphology, and reverse remodelling

Septal scar percentage, rather than global or lateral scar percentage, was significantly lower in patients with Strauss LBBB morphology (median 0%, IQR: 0–6.1%) compared with those without Strauss LBBB (median 8.8%, IQR: 0–17.0%,  $P = 0.030$ ). This was especially

pronounced in basal septal segments, with rather lower basal septal scar burden in the Strauss LBBB group [median IQR: 0% (0–2.9%) vs. 11.4% (0–20.8%),  $P = 0.019$ ; Figure 2]. In correlation analysis, myocardial scar burden correlated negatively with LVEF improvement, LVESV reduction, and LVEDD reduction (all  $P < 0.05$ ; Table 2).

Among the clinical variables, female sex, QRSD reduction, the capture of LBB, baseline LVEDD, and absence of history of atrial fibrillation were all associated with LVEF improvement, while higher baseline LVEDD displayed a negative association with a non-significant trend. The clinical parameters, coupled with CMR parameters, were included in a multivariate linear model with stepwise regression. As a result, QRSD reduction, baseline LVEDD, and septal LGE percentage were independent predictors in the final model of reverse remodelling (Table 3). Patients with significant QRSD reduction, smaller LVEDD, and lower septal LGE burden were more likely to have higher LVEF improvement.

### Prediction of response by scar burden and clinical measures

The predictive values of clinical and imaging variables for echocardiographic response, super-response, and clinical response were evaluated by ROC analyses. The clinical parameters displayed only fair to

**Table 2** Correlation analysis of CMR scar parameters and reverse remodelling

CMR variables	LVEF improvement		LVESV reduction		LVEDD reduction	
	Correlation coefficients	P-value	Correlation coefficients	P-value	Correlation coefficients	P-value
Global scar percentage, %	−0.519	<0.001	−0.572	<0.001	−0.364	0.007
Lateral scar percentage, %	−0.455	<0.001	−0.577	<0.001	−0.402	0.003
Septal scar percentage, %	−0.543	<0.001	0.580	<0.001	−0.345	0.011

Correlation coefficients were derived from Spearman's correlation analysis.

LVEDD, left ventricular end-diastolic diameter; LVEF, left ventricular ejection fraction; LVESV, left ventricular end-systolic volume (reduction calculated as percentage of change compared with baseline).

**Table 3** Univariate and multivariate linear regression analyses of baseline determinates of the left ventricular ejection fraction reduction

Variables	Univariate analysis			Multivariate analysis			
	Beta	SE	P-value	Beta	SE	VIF	P-value
Constant				38.61	11.02		<0.001
Age, years	0.232	0.149	0.126				
Male	−7.557	3.336	0.028				
Baseline QRSd, ms	0.100	0.064	0.131				
Strauss LBBB	4.519	3.597	0.215				
QRSd reduction, ms	0.213	0.095	0.030	0.174	0.086	1.089	0.048
Capture of LBB	6.937	3.354	0.044				
Stim-V6 RWPT	−0.227	0.132	0.092				
Baseline LVEDD, mm	−0.488	0.181	0.009	−0.409	0.166	1.085	0.017
eGFR, mL/min	−0.061	0.084	0.468				
Atrial fibrillation	−10.250	4.698	0.034				
Septal LGE percentage, (%)	−0.624	0.158	<0.001	−0.463	0.159	1.138	0.005
Global LGE percentage, (%)	−0.473	0.152	0.003				
Lateral LGE percentage, (%)	−0.288	0.108	0.010				

LGE, late gadolinium enhancement; SE, standard error; VIF, variance inflation factors; other abbreviations as in Tables 1 and 2.

moderate discrimination for predicting echocardiographic response, with AUCs around 0.7 (Figure 3 and Table 4) and held poor predictive value for super-response (AUC: Strauss LBBB 0.515, baseline LVEDD 0.661, stim-V6 RWPT 0.560, QRSd reduction 0.642, and capture of LBB 0.543). In comparison, the CMR-derived scar percentage displayed very good discriminability for identifying LBBAP-CRT echocardiographic responders, with AUC of 0.864, 0.857, and 0.822 for septal, global, and lateral LGE percentage. Using cut-off values based on the Youden index, global LGE percentage had the specificity of 92.9% and positive LR as high as 9.859, while lateral LGE percentage gives high sensitivity of 87.5% with the negative LR as low as 0.175. And at the 6.99% cut-off value for septal LGE percentage, lower septal scar burden predicted response with a sensitivity of 80% and specificity of 85.7%, with a positive LR of 5.594 and a negative LR of 0.233. Based on the cut-off values noted above, LVEF improvement as well as LVESV and LVEDD reduction were also significantly higher in those with lower global, septal, and lateral scar burden groups (see Supplementary material online, Figure S2). When further dividing patients according to Strauss LBBB and global, septal, and lateral LGE percentage (see Supplementary material

online, Figure S3), we observed that among the patients with the Strauss LBBB morphology, those having lower global, lateral, or septal scars displayed greater LVESV reduction and higher LVEF improvement as compared with the higher septal scar group, while patients who did not meet the Strauss LBBB criteria and having higher global, septal, or lateral scar tend to had less LVEF improvement and LVESV reduction as compared with those having lower scar burdens. Figure 4 illustrates examples of ECG and CMR images of responders from patients with and without Strauss LBBB morphology. Considering clinical response and super-response, the scar burden also displayed moderate-to-good predictive value, with septal LGE displaying better performance in identifying clinical responders (AUC 0.791) and global LGE demonstrating the highest AUC for predicting super-response (AUC 0.758).

### Predictive value of scar for adverse clinical outcomes

Over a median follow-up time of 20.3 (IQR: 11.5–38.7) months, 11 (20.4%) patients reached the combined endpoint of all-cause mortality

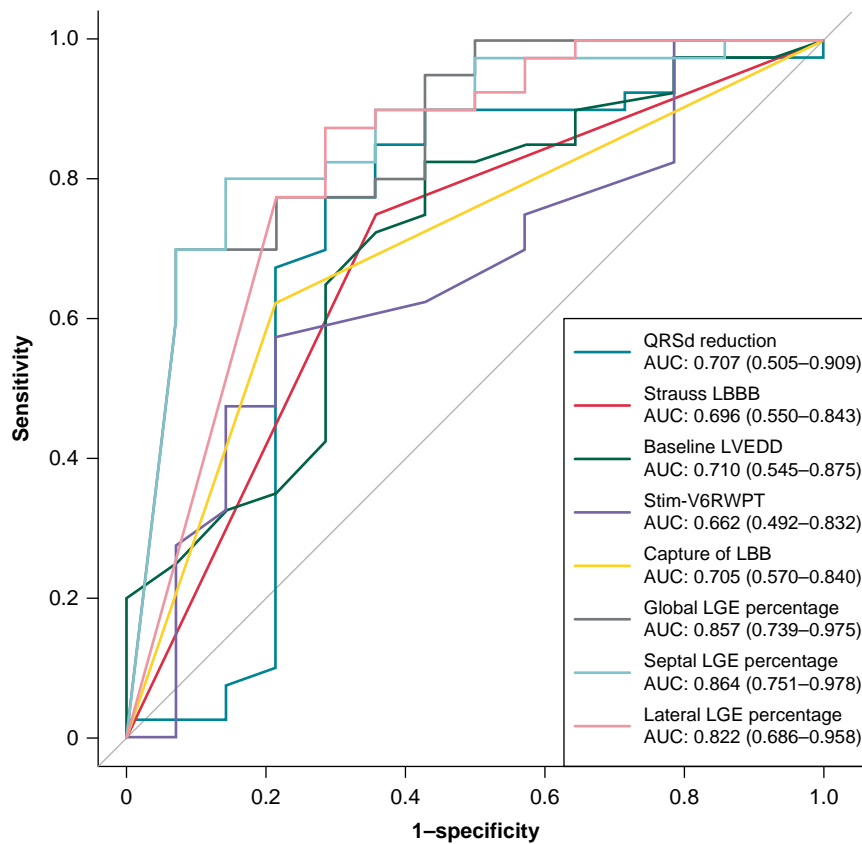


**Figure 3** Receiver operating curves of clinical and CMR parameters for predicting echocardiographic response. LBBB, left bundle branch abnormality; LBB, left bundle branch; LVEDD, left ventricular end-diastolic diameter; LGE, late gadolinium enhancement; RWPT, R wave peak time.

**Table 4** Clinical and CMR parameters for predicting echocardiographic response

Predictors	AUC (95% CI)	Cut-off	Sensitivity	Specificity	PPV	NPV	Positive LR	Negative LR
Clinical predictors								
QRSd reduction (ms)	0.707 (0.505–0.909)	24.5	0.850	0.643	0.872	0.600	2.381	0.233
Strauss LBBB	0.696 (0.550–0.843)	1	0.750	0.643	0.857	0.474	2.101	0.389
Baseline LVEDD (mm)	0.710 (0.545–0.875)	70.5	0.825	0.571	0.846	0.533	1.923	0.306
Stim-V6 RWPT (ms)	0.662 (0.492–0.832)	91.5	0.575	0.786	0.885	0.393	2.687	0.541
Capture of LBB	0.705 (0.570–0.840)	1	0.625	0.786	0.893	0.423	2.921	0.477
CMR predictors								
Global LGE percentage (%)	0.857 (0.739–0.975)	1.77	0.700	0.929	0.966	0.520	9.859	0.323
Septal LGE percentage (%)	0.864 (0.751–0.978)	6.99	0.800	0.857	0.941	0.600	5.594	0.233
Lateral LGE percentage (%)	0.822 (0.686–0.958)	0.412	0.875	0.714	0.897	0.667	3.059	0.175

AUC, area under the curve; PPV, positive predictive value; NPV, negative predictive value; LR, likelihood ratio; other abbreviations as in Tables 1 and 2.

( $n = 2$ ) or HFH ( $n = 9$ ). On Kaplan–Meier analysis, there was a significant difference in event-free survival between lower and higher scar burden groups (Figure 5). Using the same cut-off value in response analysis for global, septal, and lateral LGE percentage (1.77%, 6.99%, and 0.412%, respectively), the occurrence of the composite outcome differed significantly between patients based on global/septal/lateral scar [HR of higher global scar: 4.996; 95% confidence interval (CI): 1.078–23.151;  $P = 0.040$ ; HR of higher septal scar 4.741; 95%

CI: 1.255–17.917,  $P = 0.022$ ; HR of higher lateral scar 7.019; 95% CI: 1.838–26.806,  $P = 0.004$ ; see [Supplementary material online, Table S5](#)].

## Discussion

This study demonstrated the relationship between CMR-derived scar parameters and 6-month echocardiographic reverse remodelling, as



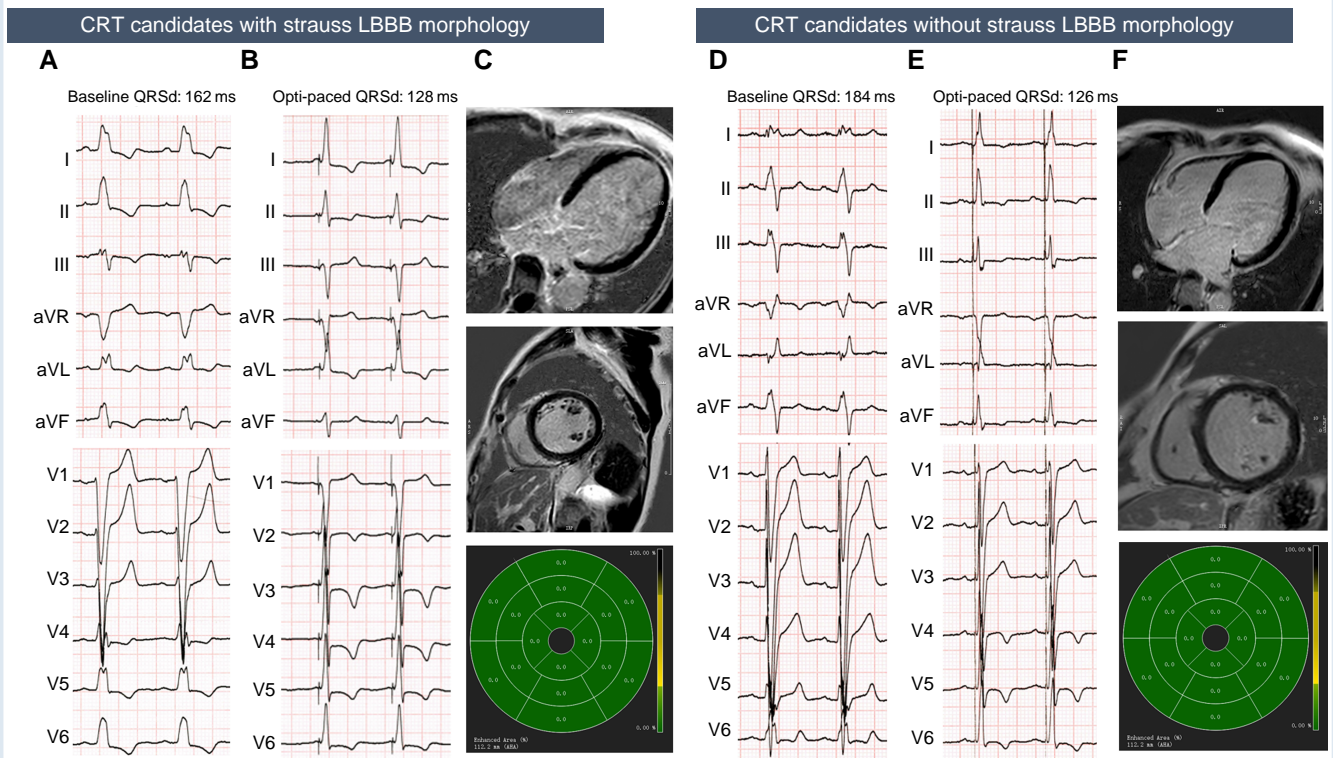


**Figure 4** Example of ECG and CMR of LBBAP-CRT responder in patients with or without Strauss LBBB. (A–C) are from an LBBAP-CRT responder with baseline ECG that shows wide QRS complex (162 ms) and meets the Strauss LBBB criteria (A). After LBBAP, optimized paced QRSd was reduced to 128 ms. (B) The LVEF recovered from 29% at baseline to 66% and LVESV reduced from 193 to 47 mL after 6 months follow-up. The CMR imaging showed no presence of LGE in the left ventricle (C). (D–F) are from an LBBAP-CRT responder with wide QRS complex (184 ms) but did not meet the Strauss LBBB criteria (D). After LBBAP-CRT, QRS complex narrowed to 126 ms (E). The LVEF improved from 26% at baseline to 48% and LVESV reduced from 112 to 48 mL after 6 months follow-up. The CMR imaging showed no presence of LGE in the left ventricle (F). CRT, cardiac resynchronization therapy; LBBB, left bundle branch abnormality; LVEDD, left ventricular end-diastolic diameter; LVEF, left ventricular ejection fraction; LVESV, left ventricular end-systolic volume; LGE, late gadolinium enhancement; opti-paced QRSd, optimized paced QRS duration.

well as clinical prognosis in patients with LBBAP-CRT. There are four important outcomes from this study: First, global, septal, and lateral scar burdens correlated negatively with reverse remodelling and displayed better performance for predicting echocardiographic response than Strauss LBBB morphology (Graphical Abstract). Second, measures of scar burden were also strong predictors of clinical outcomes after LBBAP-CRT. Third, patients with Strauss LBBB morphology tend to have lower septal scar burden compared with those without Strauss LBBB morphology. Fourth, the magnitude of reverse remodelling as measured by changes in LVEF, LVEDD, and LVESV is less in the presence of greater LV scar.

### Traditional clinical parameters

Since Huang *et al.*<sup>26</sup> reported the first successful case of LBBAP for CRT in an HF patient with LBBB in 2017, variable clinical studies have shown that the feasibility and efficacy of LBBAP are novel pacing approaches and useful for a CRT approach in patients with traditional BVP-CRT indication.<sup>10,27–30</sup> However, to date, the investigation into predictors of the LBBAP-CRT responders is limited. Although the shorter paced QRSd, greater QRSd reduction, and changes of repolarization parameters were reported to be associated with LBBAP-CRT response,<sup>31,32</sup> these indices can only be collected during or after the procedure rather than prospectively guide the optimal patient

selection. Intuitively, patients with LBBB morphology may benefit from LBBAP, given that the electrical dyssynchrony induced by LBBB can be corrected. Strauss LBBB has been considered as a predictor of ‘true’ LBBB and yielded up to 90% CRT response rate in previous studies,<sup>27,33</sup> thus being commonly recognized as an important factor in patient election for LBBAP-CRT. However, the utility of the Strauss LBBB criteria may be limited by significant interobserver variability of ECG classification.<sup>34</sup> Moreover, among patients without LBBB morphology, ~50–60% response rates were observed previously.<sup>35</sup> In our study, we observed a higher response rate of in patients with Strauss LBBB than those without (response rates: 85.7% vs. 52.6%, respectively), which re-affirms the usefulness of ECG morphology in identifying a target population who might benefit from LBBAP-CRT. However, the NPV and the specificity of this categorical parameter are only 47.4% and 64.3%, respectively, indicating that this parameter alone is insufficient. Accordingly, patients without typical LBBB morphology may also benefit from LBBAP-CRT more frequently than previously claimed. Although other clinical parameters such as baseline LVEDD and QRS reduction are associated with LVEF reduction in the current study, they are not strong of predicting the clinical response and super-response. These findings suggest that traditional clinical parameters related to electrical synchrony and echocardiographic parameters may not be sufficient to estimate response to LBBAP-CRT accurately.

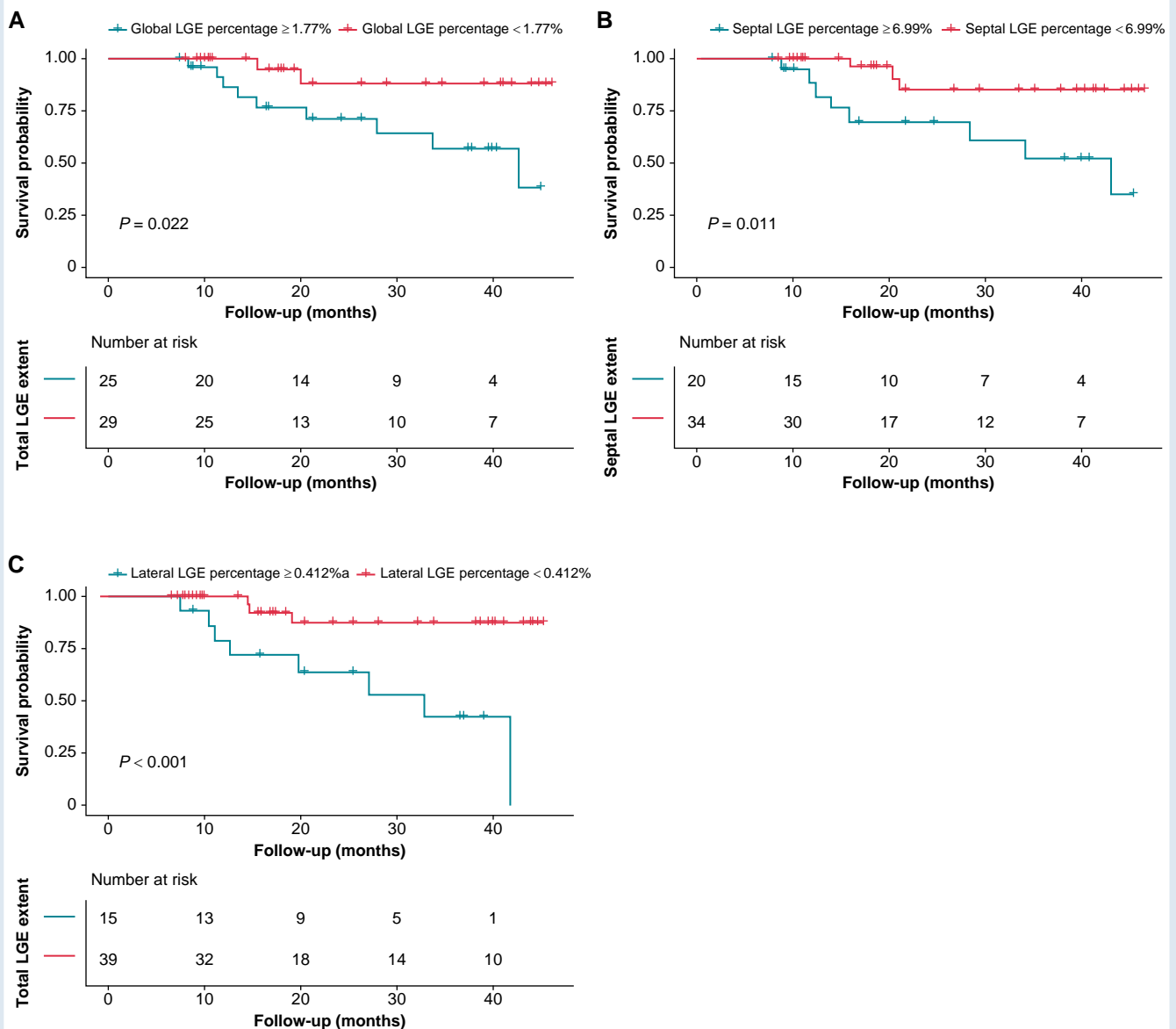


**Figure 5** Survival without composite outcomes after LBBAP-CRT in patients with lower and higher myocardial scar. Time to all-cause mortality or heart failure hospitalization according to (A) global LGE percentage, (B) septal LGE percentage, and (C) lateral LGE percentage stratified by cut-off value to predict response in ROC analysis. LGE, late gadolinium enhancement.

## Cardiovascular magnetic resonance-derived scars

Beyond the morphological and electrical characteristics, myocardial scar may also impact the effects of CRT.<sup>36,37</sup> For example, pacing over the scarred myocardial tissue in the posterolateral LV is associated with non-response to traditional BVP-CRT,<sup>13</sup> which motivated the investigations of the relationship between myocardial fibrosis and LBBAP. A previous retrospective study with small sample sizes observed that the presence and burden of septal scar is a major factor impeding lead advancement to the left bundle area. High scar burden is strongly associated with failure of LBB pacing.<sup>14</sup> Regarding the acute haemodynamic response, a small study showed that septal scar attenuated the response to LBBAP in eight patients who underwent pre-procedure CMR.<sup>38</sup> These studies suggest that scar may affect activation of the

left bundle or limit the extent of the conduction system that can activate the myocardium. The present study is the first to analyse the effect of scar features comprehensively on the prognosis after LBBAP-CRT. In this population with relatively lower global (6%) and septal scar burdens (10.7%), who have successful lead implantation in the LBB area, we observed that higher scar percentage was associated with lower likelihood of echocardiographic and clinical response. Furthermore, responders tend to have an absence or lower burden of myocardial scar, whereas non-responders have a higher burden of global, septal, and lateral scars. In multivariate linear regression, the myocardial scar percentage in septum was also strongly correlated with change of LVEF. These findings suggest that the myocardial scars limits the capacity of the LV to remodel independent of improved electrical resynchronization.

In the ROC analysis, scar burden was predictive of response and super-response, with the septal scar displaying the best predictive value

for responders (AUC of 0.864), which is higher than other clinical variables. The  $-LR$  of all the scar parameters are lower than Strauss LBBB, while the  $+LR$  are higher than Strauss LBBB, suggesting that scar parameters have stronger predictive value to classify a responder and non-responder more correctly than ECG morphology.

The assessment of clinical outcomes also indicated that a higher scar burden was associated with an increased risk of death or HFH after LBBAP-CRT. This supports the concept that the uncoupling of LBBB correction and outcome in some patients is due to the poor substrate for mechanical resynchronization. Consequently, myocardial scar is closely related to the adverse remodelling in HF and a marker of the severity of the disease. These findings highlight the prognostic value of CMR-LGE for LBBAP-CRT and suggest that myocardial fibrosis assessment may serve as a sensitive marker with higher discriminability of response and risk prediction in patients who plan to receive LBBAP-CRT. The approach of pre-procedure CMR analysis offers potential values for clinicians to improve the selection of LBBAP-CRT candidates and optimize clinical decisions.

## Limitations

The results of this study should be interpreted in light of certain methodological limitations. First, there was a relatively small sample size and this was a retrospective study. As with all retrospective studies, there may be some selection bias. Secondary, only patients with CMR examination were included in this study, which might also introduce selection bias. In our centre, CMR was routinely recommended for patients with NICM and intended for better understanding of the aetiology of cardiomyopathy. Therefore, the population evaluated was largely a non-ischæmic cohort, so the results of the present study cannot be extrapolated to ischæmic heart disease. Finally, the small number of composite events limits further multivariate adjustment of clinical parameters. Therefore, the independent effect of scar burden on echocardiographic response as well as clinical outcome should be further explored in larger populations with long-term follow-up.

## Conclusions

Lower scar burden is a strong predictor of LBBAP-CRT response. The pre-procedure CMR scar evaluation may provide useful information beyond Strauss LBBB to help clinicians for assessing potential responders to LBBAP-CRT. Future prospective studies are warranted to further explore the efficacy of pre-procedure CMR scar evaluation for optimizing the selection of LBBAP-CRT candidates in both ischæmic and non-ischæmic cohorts.

## Supplementary material

Supplementary material is available at *Europace* online.

## Acknowledgements

We thank Dr Xiaohong Zhou (Medtronic, Inc.) for his diligent review of our manuscript.

## Funding

This work was supported by the National Natural Science Foundation of China (grant number 81870260), High-level Hospital construction project of Fuwai Hospital (grant number 2022-GSP-GG-31), and CAMS Innovation Fund for Medical Sciences (grant number 2022-I2M-C&T-B-049).

**Conflict of interest:** M.R.G. is a consultant and has clinical trial support from Boston Scientific and Medtronic. The remaining authors have no conflict of interest to disclose.

## Data availability

The data will be available upon reasonable request to the corresponding author.

## References

- Kaza N, Keene D, Whinnett ZI. Generating evidence to support the physiologic promise of conduction system pacing: status and update on conduction system pacing trials. *Card Electrophysiol Clin* 2022;**14**:345–55.
- Mullens W, Auricchio A, Martens P, Witte K, Cowie MR, Delgado V et al. Optimized implementation of cardiac resynchronization therapy: a call for action for referral and optimization of care. *Europace* 2021;**23**:1324–42.
- Gold MR, Rickard J, Daubert JC, Zimmerman P, Linde C. Redefining the classifications of response to cardiac resynchronization therapy. *JACC Clin Electrophysiol* 2021;**7**:871–80.
- Chung ES, Gold MR, Abraham WT, Young JB, Linde C, Anderson C et al. The importance of early evaluation after cardiac resynchronization therapy to redefine response: pooled individual patient analysis from 5 prospective studies. *Heart Rhythm* 2022;**19**:595–603.
- Vijayaraman P, Ponnusamy S, Cano O, Sharma PS, Naperkowski A, Subposh FA et al. Left bundle branch area pacing for cardiac resynchronization therapy results from the international LBBAP collaborative study group. *JACC Clin Electrophysiol* 2021;**7**:135–47.
- Ellenbogen KA, Auricchio A, Burri H, Gold MR, Leclercq C, Leyva F et al. The evolving state of cardiac resynchronization therapy and conduction system pacing: 25 years of research at EP Europace journal. *Europace* 2023;**25**:euaad168.
- Su L, Wang S, Wu S, Xu L, Huang Z, Chen X et al. Long-term safety and feasibility of left bundle branch pacing in a large single-center study. *Circ Arrhythm Electrophysiol* 2021;**14**:e009261.
- Vijayaraman P, Herweg B, Verma A, Sharma PS, Batul SA, Ponnusamy SS et al. Rescue left bundle branch area pacing in coronary venous lead failure or nonresponse to biventricular pacing: results from International LBBAP Collaborative Study Group. *Heart Rhythm* 2022;**19**:1272–80.
- Wang Y, Zhu H, Hou X, Wang Z, Zou F, Qian Z et al. Randomized trial of left bundle branch vs biventricular pacing for cardiac resynchronization therapy. *J Am Coll Cardiol* 2022;**80**:1205–16.
- Li Y, Yan L, Dai Y, Zhou Y, Sun Q, Chen R et al. Feasibility and efficacy of left bundle branch area pacing in patients indicated for cardiac resynchronization therapy. *Europace* 2020;**22**:ii54–60.
- Liu J, Sun F, Wang Z, Sun J, Jiang X, Zhao W et al. Left bundle branch area pacing vs. biventricular pacing for cardiac resynchronization therapy: a meta-analysis. *Front Cardiovasc Med* 2021;**8**:669301.
- Aktaa S, Abidin A, Arbelo E, Burri H, Vernoooy K, Blomström-Lundqvist C et al. European Society of Cardiology Quality Indicators for the care and outcomes of cardiac pacing: developed by the Working Group for Cardiac Pacing Quality Indicators in collaboration with the European Heart Rhythm Association of the European Society of Cardiology. *Europace* 2022;**24**:165–72.
- Taylor RJ, Umar F, Panting JR, Stegemann B, Leyva F. Left ventricular lead position, mechanical activation, and myocardial scar in relation to left ventricular reverse remodeling and clinical outcomes after cardiac resynchronization therapy: a feature-tracking and contrast-enhanced cardiovascular magnetic resonance study. *Heart Rhythm* 2016;**13**:481–9.
- Ponnusamy SS, Murugan M, Ganesan V, Vijayaraman P. Predictors of procedural failure of left bundle branch pacing in scarred left ventricle. *J Cardiovasc Electrophysiol* 2023;**34**:760–4.
- Strocchi M, Gillette K, Neic A, Elliott MK, Wijesuriya N, Mehta V et al. Effect of scar and His-Purkinje and myocardium conduction on response to conduction system pacing. *J Cardiovasc Electrophysiol* 2023;**34**:984–93.
- Glikson M, Nielsen JC, Kronborg MB, Michowitz Y, Auricchio A, Barbash IM et al. 2021 ESC guidelines on cardiac pacing and cardiac resynchronization therapy. *Eur Heart J* 2021;**42**:3427–520.
- Curtis AB, Worley SJ, Adamson PB, Chung ES, Niazi I, Sherfese L et al. Biventricular pacing for atrioventricular block and systolic dysfunction. *N Engl J Med* 2013;**368**:1585–93.
- Strauss DG, Selvester RH, Wagner GS. Defining left bundle branch block in the era of cardiac resynchronization therapy. *Am J Cardiol* 2011;**107**:927–34.
- Pujol-López M, Ferró E, Borràs R, Garre P, Guasch E, Jiménez-Arjona R et al. Stepwise application of ECG and electrogram-based criteria to ensure electrical resynchronization with left bundle branch pacing. *Europace* 2023;**25**:euaad128.
- Burri H, Jastrzebski M, Cano Ó, Čurilica K, de Pooter J, Huang W et al. EHRA clinical consensus statement on conduction system pacing implantation: endorsed by the Asia Pacific Heart Rhythm Society (APHRS), Canadian Heart Rhythm Society (CHRS), and Latin American Heart Rhythm Society (LAHRS). *Europace* 2023;**25**:1208–36.
- Iles LM, Ellims AH, Llewellyn H, Hare JL, Kaye DM, McLean CA, et al. Histological validation of cardiac magnetic resonance analysis of regional and diffuse interstitial myocardial fibrosis. *European Heart Journal - Cardiovascular Imaging* 2015;**16**:14–22. <https://doi.org/10.1093/ehjci/jeu182>

22. Ypenburg C, van Bommel RJ, Borleffs CJW, Bleeker GB, Boersma E, Schalij MJ et al. Long-term prognosis after cardiac resynchronization therapy is related to the extent of left ventricular reverse remodeling at midterm follow-up. *J Am Coll Cardiol* 2009;**53**:483–90.
23. Parreira L, Tsyganov A, Artyukhina E, Vernooy K, Tondo C, Adragao P et al. Non-invasive three-dimensional electrical activation mapping to predict cardiac resynchronization therapy response: site of latest left ventricular activation relative to pacing site. *Europace* 2023;**25**:1458–66.
24. Vijayaraman P, Herweg B, Ellenbogen KA, Gajek J. His-optimized cardiac resynchronization therapy to maximize electrical resynchronization: a feasibility study. *Circ Arrhythm Electrophysiol* 2019;**12**:e006934.
25. Van BRJ, Mollema SA, Borleffs CJW, Bertini M, Ypenburg C, Marsan NA et al. Impaired renal function is associated with echocardiographic nonresponse and poor prognosis after cardiac resynchronization therapy. *J Am Coll Cardiol* 2011;**57**:549–55.
26. Huang W, Su L, Wu S, Xu L, Xiao F, Zhou X et al. A novel pacing strategy with low and stable output: pacing the left bundle branch immediately beyond the conduction block. *Can J Cardiol* 2017;**33**:1736.e1–e3.
27. Huang W, Wu S, Vijayaraman P, Su L, Chen X, Cai B et al. Cardiac resynchronization therapy in patients with nonischemic cardiomyopathy using left bundle branch pacing. *JACC Clin Electrophysiol* 2020;**6**:849–58.
28. Salden FCWM, Luermans JGLM, Westra SW, Weijs B, Engels EB, Heckman LIB et al. Short-term hemodynamic and electrophysiological effects of cardiac resynchronization by left ventricular septal pacing. *J Am Coll Cardiol* 2020;**75**:347–59.
29. Chen X, Ye Y, Wang Z, Jin Q, Qiu Z, Wang J et al. Cardiac resynchronization therapy via left bundle branch pacing vs. optimized biventricular pacing with adaptive algorithm in heart failure with left bundle branch block: a prospective, multi-centre, observational study. *Europace* 2022;**24**:807–16.
30. Jastrzębski M, Kielbasa G, Cano O, Curila K, Heckman L, De Pooter J et al. Left bundle branch area pacing outcomes: the multicentre European MELOS study. *Eur Heart J* 2022;**43**:4161–73.
31. Li Y, Lu W, Hu Q, Cheng C, Lin J, Zhou Y et al. Changes of repolarization parameters after left bundle branch area pacing and the association with echocardiographic response in heart failure patients. *Front Physiol* 2022;**13**:912126.
32. Guan XM, Li DN, Zhao FL, Zhao YN, Yang YH, Dai BL et al. Short QRS duration after His-Purkinje conduction system pacing predicts left ventricular complete reverse remodeling in patients with true left bundle branch block and heart failure. *Front Cardiovasc Med* 2022;**9**:824194.
33. Wu S, Su L, Vijayaraman P, Zheng R, Cai M, Xu L et al. Left bundle branch pacing for cardiac resynchronization therapy: nonrandomized on-treatment comparison with his bundle pacing and biventricular pacing. *Can J Cardiol* 2021;**37**:319–28.
34. van Stipdonk AMW, Vanbelle S, Ter Horst IAH, Luermans JG, Meine M, Maass AH et al. Large variability in clinical judgement and definitions of left bundle branch block to identify candidates for cardiac resynchronisation therapy. *Int J Cardiol* 2019;**286**: 61–5.
35. Ezzeddine FM, Pistiolis SM, Pujol-Lopez M, Lavelle M, Wan EY, Patton KK et al. Outcomes of conduction system pacing for cardiac resynchronization therapy in patients with heart failure: a multicenter experience. *Heart Rhythm* 2023;**20**: 863–71.
36. Ahmed W, Samy W, Tayeh O, Behairy N, Abd El Fattah A. Left ventricular scar impact on left ventricular synchronization parameters and outcomes of cardiac resynchronization therapy. *Int J Cardiol* 2016;**222**:665–70.
37. Aalen JM, Donal E, Larsen CK, Duchenne J, Lederlin M, Cvijic M et al. Imaging predictors of response to cardiac resynchronization therapy: left ventricular work asymmetry by echocardiography and septal viability by cardiac magnetic resonance. *Eur Heart J* 2020;**41**:3813–23.
38. Elliott MK, Strocchi M, Sieniewicz BJ, Sidhu B, Mehta V, Wijesuriya N et al. Biventricular endocardial pacing and left bundle branch area pacing for cardiac resynchronization: mechanistic insights from electrocardiographic imaging, acute hemodynamic response, and magnetic resonance imaging. *Heart Rhythm* 2023;**20**:207–16.